ACS OMEGA

http://pubs.acs.org/journal/acsodf

Article

Zeolitic Imidazolate Frameworks as Latent Thermal Initiators in the Curing of Epoxy Resin

Osamu Shimomura,* Hiroshi Furuya, Daiki Fukumoto, Atsushi Ohtaka, and Ryôki Nomura

Cite This: *ACS Omega* 2021, 6, 30292−30297

Read Online

ACCESS | Metrics & More | Article Recommendations | Supporting Information

ABSTRACT: The curing of a mixture of glycidyl phenyl ether (GPE) and hexahydro-4-methylphthalic anhydride (MHHPA) with zeolitic imidazolate frameworks (ZIFs)—ZIF-7, ZIF-8, ZIF-11, and ZIF-14—as latent thermal initiators has been critically evaluated. For ZIF-8 and ZIF-14, the % conversion values for GPE were 92 and 93%, respectively, for curing at 100 °C and for 1 h. With regard to the stability of ZIF-8 and ZIF-14 in the GPE-MHHPA mixture, the % conversion values for GPE were 11 and 12% for storage over 8 days at 25 °C. The ZIF-8 and ZIF-14 initiators exhibited excellent thermal latency for heating at 100 °C and showed good stability for storage at 25 °C. To evaluate the practicality of the resin curing system, the reactions of 2,2-bis(4-glycidyloxyphenyl)propane (DGEBA) and MHHPA with ZIFs were studied by differential scanning calorimetry. Prominent exothermic peaks for ZIF-8 and ZIF-14 were observed at 157 and 162 °C, respectively; by comparison, for the commercially available microencapsulated latent thermal initiators HX-3088 and HX-3722, the respective peak maxima were 177 and 181 °C, respectively. The exothermic peak maxima for ZIF-8 and ZIF-14 were lower than those for HX-3088 and HX-3722. The ZIF-8 and ZIF-14 initiators can be stored in precured epoxy resin at 25 °C and cured by lower temperatures compared with commercially-available initiators HX-3088 and HX-3722.

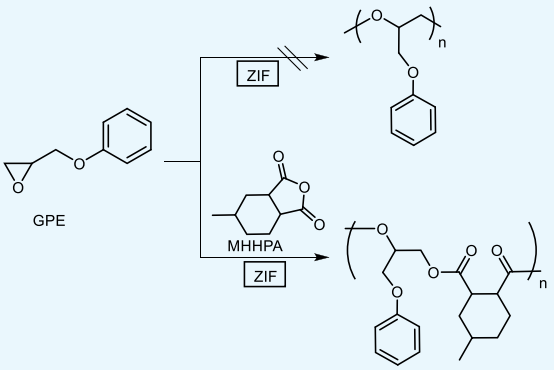

1. INTRODUCTION

Zeolitic imidazolate frameworks (ZIFs) are porous materials formed by coordination of metal cations with imidazolates.[1−4] The coordination angle of the metal cations and the imidazolate anions in the ZIFs is approximately 145°, an angle that is similar to that for the Si−O−Si bond in silica and zeolite.[3] As a result, ZIFs are stable under high temperature and relatively harsh chemical conditions. For example, Park et al. reported the synthesis of 12 types of ZIFs and studied their thermal and chemical stabilities.[4] Among them, zeolitic imidazolate framework-8 (ZIF-8) formed a sodalite structure with zinc cations and 2-methylimidazolate, which was very stable in boiling organic solvents and boiling sodium hydroxide solution. Recently, numerous applications of ZIFs have been reported. Zhuang et al. reported the release behavior of fluorescein encapsulated in the pores of ZIF-8 in pH 7.4 phosphate-buffered saline (PBS) and pH 6.0 buffered solution.[5] A release of less than 10% of the encapsulated fluorescein was detected in PBS, whereas 50% was released in the pH 6.0 buffered solution within 1 h. The outer structure of ZIF-8 collapsed after 1 h because of the dissociation of the bonds between zinc cations and 2-methylimidazolate under acidic conditions. Nanocomposite materials consisting of epoxy resin and ZIFs have been studied on account of the high functionality of polymer materials.[6−9] For example, Liu et al. focused on reducing the dielectric constant of epoxy resins using ZIF-8 as a curing agent.[6] With respect to the curing temperature of epoxy resin with ZIF-8, an exothermic peak was observed at 215 °C while using 2-methylimidazole at 110 °C as determined by differential scanning calorimetry (DSC). The reaction mechanism was considered to involve the participation of the low-reactivity 2-methylimidazolate moiety in the structure of ZIF-8 as a result of electron withdrawal by cationic zinc. In the present work, the curing reaction of bisphenol A diglycidyl ether epoxy resin is the focus of research. We have already reported that intercalated imidazoles within zirconium phosphate (α-ZrP) were utilized as latent thermal initiators in the reaction of epoxy resins.[10−15] Among them, 2-methylimidazole (2MIm)-intercalated α-ZrP (α-ZrP·2MIm) exhibits excellent stability during storage at 25 °C and high reactivity under appropriate heating conditions. For the reaction of glycidyl phenyl ether (GPE) and hexahydro-4-methylphthalic anhydride (MHHPA) with α-ZrP·2MIm as a latent thermal initiator, the % conversion for the reaction was 89% at 120 °C for 1 h, whereas it was 67% at 100 °C for 1 h. When using a latent thermal initiator for curing of epoxy resins, a heating

Received: May 19, 2021
Accepted: October 21, 2021
Published: November 1, 2021

temperature as low as possible should be used for curing. Also, with respect to the storage of epoxy resin, it is desirable to maintain a high stability for the precured resins for as long a time as possible. In this study, the curing behavior of a mixture of DGEBA and MHHPA epoxy resins with ZIFs as latent thermal initiators is evaluated.

2. RESULTS AND DISCUSSION

Epoxy resins using acid anhydrides as curing agents are used for the preparation of electrical insulating materials. Among them, hexahydro-4-methylphthalic anhydride (MHHPA) is a colorless and transparent liquid and has the advantage of ease of handling in the curing process. Liu et al. examined the curing behavior of DGEBA with ZIF-8 by DSC measurement, and an exothermic peak was observed at 215 °C.[6] To avoid thermal hysteresis under high temperature, we attempted to use an acid anhydride as a curing agent in the curing of epoxy resin. For this, the catalytic activity of ZIFs in the copolymerization reaction of GPE and MHHPA as the curing model was evaluated. To this end, the reaction of a mixture of GPE-MHHPA with ZIF-8 (3 mol % of 2-methylimidazolate content for GPE) was investigated for temperatures ranging from 60 to 120 °C for 1 h. The results are presented in Figure 1, and it may be observed that the reaction did not proceed at

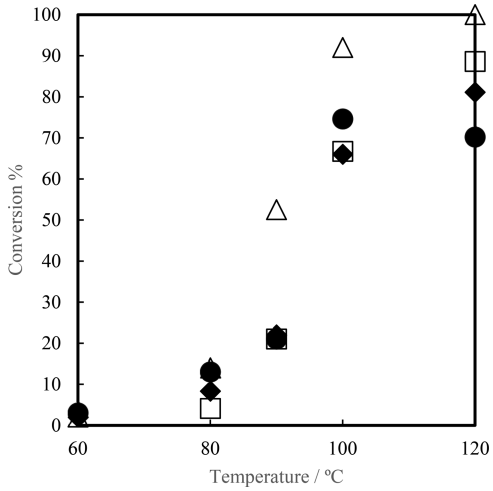

Figure 1. Percent conversion of GPE as a function of temperature for the reaction (1 h) of GPE-MHHPA with ZIF-8 (unshaded triangles), α-ZrP·2MIm (unshaded squares),[10] HX-3088 (shaded diamonds),[10] and HX-3722 (shaded circles).[10]

60 °C, whereas at 100 °C the % conversion reached 92%. It has been reported that for the latent thermal initiator 2MIm-intercalated zirconium phosphate (α-ZrP·2MIm) and the commercially available latent thermal initiators HX-3088 and HX-3722, the % conversion values were 67% (α-ZrP·2MIm), 66% (HX-3088), and 75% (HX-3722), respectively.[10] In the present study, the use of ZIF-8 at 100 °C gave the highest % conversion value. In comparison, the % conversion value for ZIF-8 at 90 °C was 53%. Clearly, the curing of epoxy resin at relatively low temperatures, e.g., 90 °C, can be expected. The % conversion values for GPE with ZIF-8 at 90 °C over 1−3 h are presented in Figure 2. It can be seen that the % conversion values increased with increasing reaction time and reached 94% after 3 h. The molecular weight of the polymer obtained with ZIF-8 for the curing reaction at 120 °C and for 1 h was measured by GPC. The number average molecular weight and

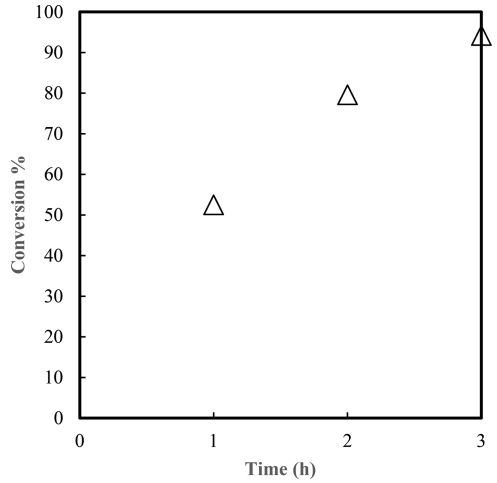

Figure 2. Percent conversion for GPE as a function of time for the reaction of GPE-MHHPA with ZIF-8 at 90 °C.

the molecular weight distribution were M_n = 2500 and M_w/M_n = 1.3, respectively. To confirm the degradation of ZIF-8 in the reaction of GPE-MHHPA at 120 °C for 1 h, the polymer products obtained were dissolved in THF. The THF solution was filtered by a membrane filter, and the remaining ZIF-8 was hardly recovered due to the homogeneous reaction under heating conditions.

The stability of the latent thermal initiator in the epoxy resin at typical storage temperatures is also an important aspect of the chemical reactivity that needs to be investigated. The % conversion values for GPE with ZIF-8, α-ZrP·2MIm, HX-3088, and HX-3722 were investigated at 25 °C as shown in Figure 3.

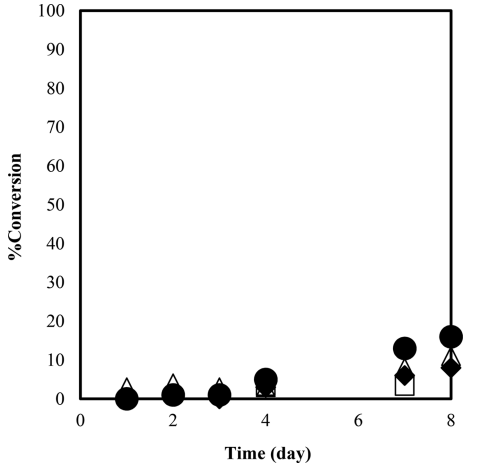

Figure 3. Percent conversion for GPE as a function of time for the reaction of GPE-MHHPA with ZIF-8 (unshaded triangles), α-ZrP·2MIm (unshaded squares), HX-3088 (shaded diamonds), and HX-3722 (shaded circles) at 25 °C.

The % conversion values over 7 days were 8% for ZIF-8, 3% for α-ZrP·2MIm, 6% for HX-3088, and 13% for HX-3722, respectively. The initiator ZIF-8 shows adequate stability for storage at 25 °C and high reactivity at 90 °C. Thus, the zeolitic imidazolate framework of ZIF-8 can be considered to exhibit excellent latent thermal initiation performance in the GPE-MHHPA reaction system. The reactivity of GPE-MHHPA with the imidazolates ZIF-7, ZIF-11, and ZIF-14 under various heating regimes for 1 h are shown in Figure 4. None of these

https://doi.org/10.1021/acsomega.1c02619
ACS Omega 2021, 6, 30292−30297

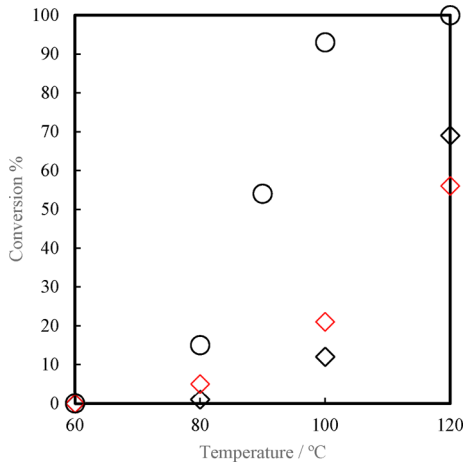

Figure 4. Percent conversion for GPE as a function of temperature for the reaction (1 h) with ZIF-7 (black unshaded diamonds), ZIF-11 (red unshaded diamonds), and ZIF-14 (black unshaded circles).

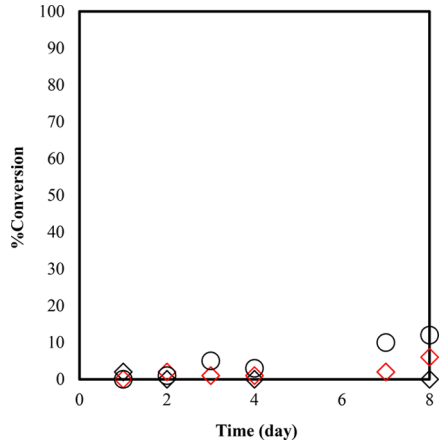

Figure 5. Percent conversion for GPE as a function of time for the reaction of GPE-MHHPA with ZIF-7 (black unshaded diamonds), ZIF-11 (red unshaded diamonds), and ZIF-14 (black unshaded circles) at 25 °C.

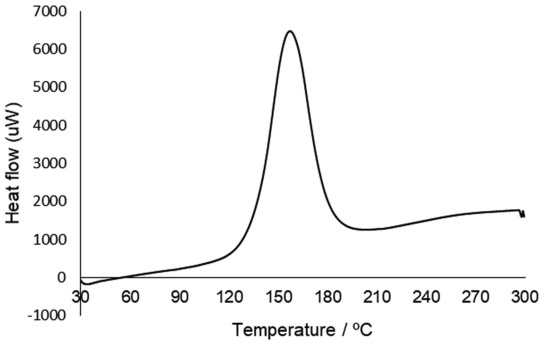

Figure 6. DSC results for DGEBA-MHHPA with ZIF-8.

Table 1. Onset, Peak Maximum, and Offset Temperatures from DSC Curves for Different Curing Agents

curing agent	onset T (°C)	peak maximum T (°C)	offset T (°C)
ZIF-7	135	172	202
ZIF-8	127	157	183
ZIF-11	146	172	202
ZIF-14	136	162	184
2MIm	122	148	169
2EIm[a]	121	147	171
BIm[b]	128	156	171
HX3088	138	177	203
HX3722	141	181	205
α-ZrP·2MIm	123	162	184

[a]2-Ethylimidazole. [b]Benzimidazole.

ZIFs exhibited reactivity at 60 °C. The % conversion value for GPE with ZIF-14 was 93% for a 1 h reaction at 100 °C. The alkyl imidazolate compounds ZIF-8 and ZIF-14 showed similar reactivity for the reaction of GPE-MHHPA. In the case of the benzimidazolate compounds ZIF-7 and ZIF-11, the % conversion values were 12 and 21% for 1 h and 100 °C, respectively. The reactivities of ZIF-7 and ZIF-11 were lower compared with ZIF-8 and ZIF 14 presumably because of the low nucleophilicity of the benzimidazole moiety of ZIF-7 and ZIF-11. In the Knoevenagel reaction of benzaldehyde and malononitrile using ZIF-8 as catalysts, the smaller-size catalysts exhibited higher catalytic activity because of the increased external surface of small crystals.[16] It was hoped that by altering the particle sizes in ZIF-7 (75 nm) and ZIF-11 (6.5 μm), there would be changes in reactivity, but this proved not to be the case. Given that the reaction of GPE-MHHPA proceeds after the degradation of the ZIFs, the reactivity may not be affected by the particle size in the ZIFs. Different sizes of 100 nm[6] and 500 nm[16] of ZIF-8 were prepared, and their reactivity was compared to ZIF-8 (280 nm) as mentioned above. These differences in ZIF-8 sizes were not observed for the reactivity of GPE-MHHPA.

With regard to the stability of ZIF-14 in GPE-MHHPA at 25 °C, the % conversion value was 10% for 7 days of storage as shown in Figure 5. The stabilities of ZIF-7, ZIF-11, and ZIF-14 were also found to be acceptable at 25 °C.

The model reaction of the epoxy resin using the monofunctional epoxy compound of GPE as the epoxy monomer and the subsequent curing of GPE-MHHPA with ZIF-8 and ZIF-14 showed good performance. The practicality of reacting the bifunctional epoxy compound of 2,2-bis(4-glycidyloxyphenyl)-propane (DGEBA) and MHHPA with ZIFs was evaluated by DSC. The exothermic peak observed during the progress of the reaction was examined. The DSC response curve for DGEBA-MHHPA with ZIF-8 as curing agent is presented in Figure 6, where it may be seen that the onset, peak maximum, and offset temperatures occurred at 127, 157, and 183 °C, respectively. Table 1 summarizes these temperatures for the selected ZIFs and structural component imidazoles as curing agents. The temperatures at the peak maxima for the ZIFs were adopted as the curing temperatures. The order of these temperatures (lowest to highest) was as follows: ZIF-8 < ZIF-14 < ZIF-7 = ZIF-11. The order obtained by DSC was similar to the order for the GPE-MHHPA systems as determined by ^{1}H-NMR analyses. The differences in the sizes of the crystal structures of ZIF-7 and ZIF-11 did not result in differences in the respective peak maxima temperatures, both values being 172 °C. The temperatures for the peak maxima with 2MIm, 2-ethylimidazole (2EIm), and benzimidazole (BIm) were lower than those for the corresponding ZIFs. Comparing the exothermic peak maxima for ZIF-8 and ZIF-14 with those for the microcapsule-type latent curing agents HX3088 and HX3722, the exothermic peaks for ZIF-8 at 157 °C and ZIF-14 at 162 °C were lower than those for HX3088 at 177 °C and HX3722 at 181 °C. To conclude, ZIF-8 and ZIF-14 gave

https://doi.org/10.1021/acsomega.1c02619
ACS Omega 2021, 6, 30292−30297

excellent performance as latent thermal initiators in the curing of epoxy resin.

The tan δ values obtained from the DMA measurements for DGEBA-MHHPA are plotted as a function of temperature for ZIF-8 and 2MIm in Figure 7. The temperature at the peak

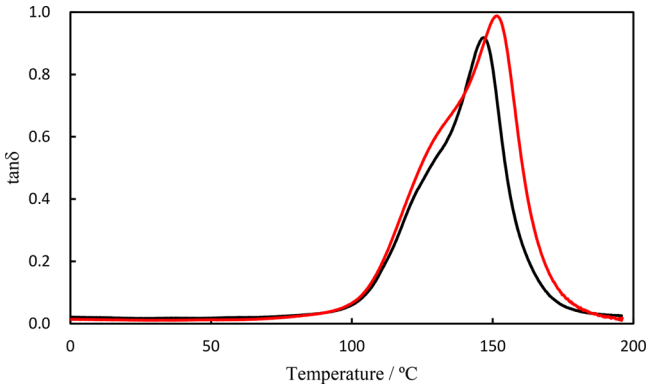

Figure 7. Tan δ from DMA plots for DGEBA-MHHPA as a function of temperature with ZIF-8 (red line) and 2MIm (black line).

maximum (T_g) was 152 °C for ZIF-8 and 147 °C for 2MIm. The storage modulus for DGEBA-MHHPA cured with ZIF-8 and 2MIm is shown in Figure 8. No significant differences

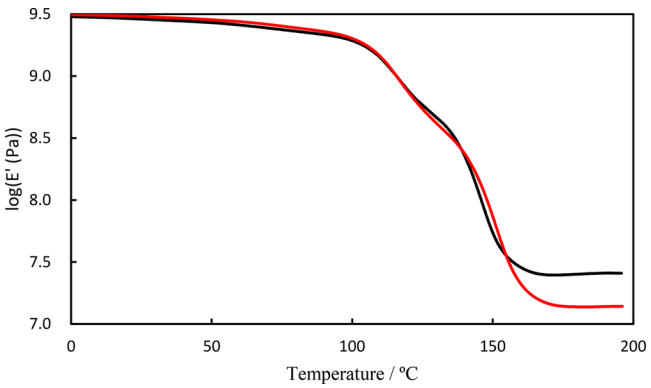

Figure 8. Storage modulus from DMA plots for DGEBA-MHHPA as a function of temperature with ZIF-8 (red line) and 2MIm (black line).

were observed below T_g at 152 °C. The storage modulus over T_gs at 180 °C and the log E' with ZIF-8 and 2MIm were 7.40 (25.2 MPa) and 7.14 (13.7 MPa), respectively. The difference of 11.5 MPa in the E' values might have originated from the density of the cured DGEBA-MHHPA as a result of cross-linking. Optical images of the cured resins of DGEBA-MHHPA with ZIF-8 and α-ZrP·2MIm are presented in Figure 9. As a result of a residue of the inorganic filler α-ZrP remaining in the cured resin, the image was cloudy. However,

Figure 9. Optical image of DGEBA-MHHPA cured with ZIF-8 (left) and α-ZrP·2MIm (right).

the resin cured with ZIF-8 was transparent, and residual ZIF-8 was not observed.

A plausible reaction mechanism for DGEBA-MHHPA with ZIF-8 is outlined in Figure 10. The small number of acidic protons from the carboxylic acid of the hydrolyzed anhydride of MHHPA may accelerate the degradation of ZIF-8. To avoid the impurity of carboxylic acid in MHHPA, purified MHHPA by vacuum distillation was used in the polymerization of GPE-MHHPA with ZIF-8, and the conversions were 33, 89, and 90% at 90, 100, and 120 °C for 1 h. In the polymerization with unpurified MHHPA, the conversions were 53, 92, and > 99% at 90, 100, and 120 °C for 1 h as shown in Figure 1. The conversions decreased especially at 80 °C from 53 to 33%, but the reaction could not be stopped in the polymerization. ZIFs might be decomposed under heating conditions to generate very small amounts of carboxylic acid by impure water. The generated 2-methylimidazole attached to MHHPA may react with GPE to generate the corresponding cured products.

3. EXPERIMENTAL SECTION

3.1. Materials. Glycidyl phenyl ether (GPE), hexahydro-4-methylphthalic anhydride (MHHPA), and 2,2-bis(4-glycidyloxyphenyl)propane (DGEBA) were purchased from Tokyo Chemical Industries, Co., Ltd. (Tokyo, Japan). Zeolitic imidazolate frameworks comprising ZIF-8,[17] ZIF-14,[18] ZIF-7,[19] and ZIF-11[20] were prepared as described elsewhere. Solvents and other chemicals were used as received without further purification. The mold releasing agent, Daifree GA-7500, was purchased from Daikin Industries Ltd. (Osaka, Japan). The microencapsulated latent thermal initiators, HX-3088 and HX-3722, were obtained from Asahi Kasei Co. Ltd. (Tokyo, Japan).

3.2. Measurements. X-ray diffraction (XRD) spectra were recorded using a Rigaku RINT2200 spectrometer (Tokyo, Japan) under the following operating conditions: Cu K_α radiation of 40 kV, 40 mA over a scan range of 3−40° at a rate of 2° min^{-1}. NMR spectra were obtained using a JEOL JNM-ECZS (400 MHz) spectrometer (Tokyo, Japan) with tetramethylsilane (TMS) as an internal standard. Fourier transform infrared spectroscopy (FT-IR) measurements were carried out with an Alpha spectrometer (Billerica, MA, USA). Scanning electron microscopy (SEM) images were obtained using a JEOL JSM-840 (Tokyo, Japan) and a Zeiss Auriga (Oberkochen, Germany). Differential scanning calorimetry (DSC) was carried out with a Hitachi DSC7020 (Tokyo, Japan) at a heating rate of 10 °C min^{-1} under nitrogen. Gel permeation chromatography (GPC) was performed with a Shimadzu 20A (Tokyo, Japan, Shodex KF-804 L, KF805L, and KF806L; THF as eluent) using polystyrene standards. Dynamic mechanical analyses (DMA) were performed with a Hitachi DMA7100 thermal analysis system (Tokyo, Japan) in tensile mode at a frequency of 1 Hz and with a heating rate of 3 °C min^{-1} from −20 to 200 °C.

3.3. Typical Polymerization Procedure. A mixture of GPE (151 mg, 1.0 mmol), MHHPA (168 mg, 1.0 mmol), and ZIF-8 (3.4 mg, 0.015 mmol) was stirred with a stirring bar at ambient temperature. The reaction was carried out for 1 h while stirring in an oil bath preheated at 80 °C. A small aliquot of the reaction mixture was dissolved in $CDCl_3$, and an ^{1}H-NMR spectrum was acquired to determine the extent of conversion of GPE.

3.4. Measurement of Molecular Weight and Molecular Weight Distribution. A mixture of GPE (1.50 g, 10.0

https://doi.org/10.1021/acsomega.1c02619
ACS Omega 2021, 6, 30292−30297

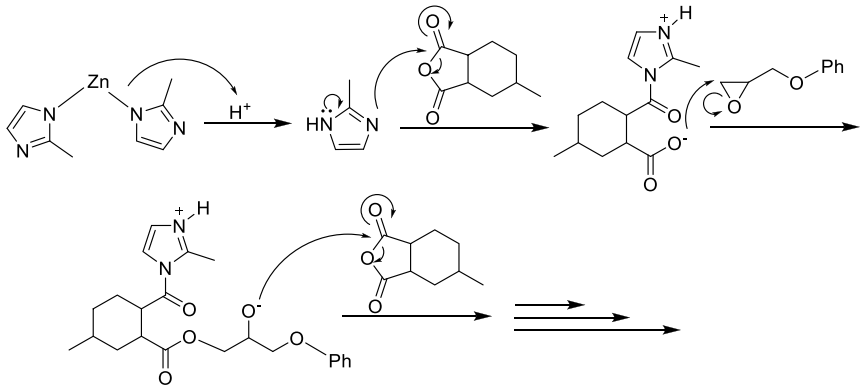

Figure 10. Plausible reaction mechanism for DGEBA-MHHPA with ZIF-8.

mmol), MHHPA (1.68 g, 10.0 mmol), and ZIF-8 (34.1 mg, 0.15 mmol) was stirred by stirring bar at ambient temperature. The reaction was carried out for 1 h while stirring in an oil bath preheated at 120 °C. After the reaction, tetrahydrofuran (THF, 5 mL) was added to the mixture. The polymer was precipitated from the THF solution with methanol and dried under a vacuum (48% yield). The molecular weight was determined by GPC analysis (M_n = 2500, M_w/M_n = 1.3). Molecular weights with ZIF-14 (M_n = 2400, M_w/M_n = 1.2), ZIF-7 (M_n = 2600, M_w/M_n = 1.3), and ZIF-11 (M_n = 2700, M_w/M_n = 1.3) were determined by similar procedures.

3.5. Particle Size Measurement for ZIFs. The average particle sizes for the ZIFs were determined from inspection of the SEM images and were based on measurement of the diameters of five particles selected at random. The average particle sizes for ZIF-8, ZIF-14, ZIF-7, and ZIF-11 were 280 nm, 2.1 μm, 75 nm, and 6.5 μm, respectively.

3.6. Preparation of Cured Epoxy Resin for DMA Measurement. The cured epoxy resins with ZIF-8 were prepared as follows: A mixture of DGEBA (342 mg, 1 mmol), MHHPA (336 mg, 2.0 mmol), and ZIF-8 (7.0 mg, 0.031 mmol) was stirred in a preheated oil bath at 90 °C for 30 min. The mixture was then poured onto a glass slide enclosed with masking tape (4 cm × 5 mm) and coated with a mold-releasing agent. The resin on the glass slide was kept under reduced pressure at ambient temperature for 1 h. After degassing, reaction of the precured resin was allowed to proceed for 1 h at 100 °C.

■ ASSOCIATED CONTENT

Supporting Information

The Supporting Information is available free of charge at https://pubs.acs.org/doi/10.1021/acsomega.1c02619.

Preparation, XRD patterns, and SEM images of ZIF-8, ZIF-14, ZIF-7, and ZIF-11 (PDF)

■ AUTHOR INFORMATION

Corresponding Author

Osamu Shimomura − *Department of Applied Chemistry, Osaka Institute of Technology, Osaka 535-8585, Japan;* orcid.org/0000-0001-6563-9743; Email: osamu.shimomura@oit.ac.jp

Authors

Hiroshi Furuya − *Department of Applied Chemistry, Osaka Institute of Technology, Osaka 535-8585, Japan*

Daiki Fukumoto − *Department of Applied Chemistry, Osaka Institute of Technology, Osaka 535-8585, Japan*

Atsushi Ohtaka − *Department of Applied Chemistry, Osaka Institute of Technology, Osaka 535-8585, Japan;* orcid.org/0000-0001-8518-5187

Ryôki Nomura − *Department of Applied Chemistry, Osaka Institute of Technology, Osaka 535-8585, Japan*

Complete contact information is available at: https://pubs.acs.org/10.1021/acsomega.1c02619

Notes

The authors declare no competing financial interest.

■ ACKNOWLEDGMENTS

This work was supported by the research project of Osaka Institute of Technology.

■ REFERENCES

(1) Banerjee, R.; Phan, A.; Wang, B.; Knobler, C.; Furukawa, H.; O'Keeffe, M.; Yaghi, O. M. High-Throughput Synthesis of Zeolitic Imidazolate Frameworks and Application to CO2 Capture. *Science* **2008**, *319*, 939−943.

(2) Phan, A.; Doonan, C. J.; Uribe-Romo, F. J.; Knobler, C. B.; O'Keeffe, M.; Yaghi, O. M. Synthesis, Structure, and Carbon Dioxide Capture Properties of Zeolitic Imidazolate Frameworks. *Acc. Chem. Res.* **2010**, *43*, 58−67.

(3) Li, K.; Olson, D. H.; Seidel, J.; Emge, T. J.; Gong, H.; Zeng, H.; Li, J. Zeolitic Imidazolate Frameworks for Kinetic Separation of Propane and Propene. *J. Am. Chem. Soc.* **2009**, *131*, 10368−10369.

(4) Park, K. S.; Ni, Z.; Cote, A. P.; Choi, J. Y.; Huang, R.; Uribe-Romo, F. J.; Chae, H. K.; O'Keeffe, M.; Yaghi, O. M. Exceptional chemical and thermal stability of zeolitic imidazolate frameworks. *Proc. Natl. Acad. Sci. U. S. A.* **2006**, *103*, 10186−10191.

(5) Zhuang, J.; Kuo, C.-H.; Chou, L.-Y.; Liu, D.-Y.; Weerapana, E.; Tsung, C.-K. Optimized Metal-Organic-Framework Nanospheres for Drug Delivery: Evaluation of Small-Molecule Encapsulation. *ACS Nano* **2014**, *8*, 2812−2819.

(6) Liu, C.; Mullins, M.; Hawkins, S.; Kotaki, M.; Sue, H. J. Epoxy Nanocomposites Containing Zeolitic Imidazolate Framework-8. *ACS Appl. Mater. Interfaces* **2018**, *10*, 1250−1257.

(7) Liu, C.; Zhang, T.; Daneshvar, F.; Feng, S.; Zhu, Z.; Kotaki, M.; Mullins, M.; Sue, H.-J. High dielectric constant epoxy nanocomposites based on metal organic frameworks decorated multi-walled carbon nanotubes. *Polymer* **2020**, *207*, 122913.

(8) Lee, S. H.; Seo, H. Y.; Yeom, Y. S.; Kim, J. E.; An, H.; Lee, J.-S.; Jeong, H.-K.; Baek, K.-Y.; Cho, K. Y.; Yoon, H. G. Rational design of epoxy/ ZIF-8 nanocomposites for enhanced suppression of copper ion migration. *Polymer* **2018**, *150*, 159−168.

(9) Zhan, Y.; Wang, Y.; Wang, M.; Ding, X.; Wang, X. Improving the Curing and Mechanical Properties of Short Carbon Fibers/Epoxy Composites by Grafting Nano ZIF-8 on Fibers. *Adv. Mater. Interfaces* **2020**, *7*, 1901490.
(10) Shimomura, O.; Tokizane, K.; Nishisako, T.; Yamaguchi, S.; Ichihara, J.; Kirino, M.; Ohtaka, A.; Nomura, R. Imidazoles-intercalated α-zirconium phosphate as latent thermal initiators in the reaction of glycidyl phenyl ether (GPE) and hexahydro-4-methylphthalic anhydride (MHHPA). *Catalysts* **2017**, *7*, 172/1−172/11.
(11) Shimomura, O.; Suetou, R.; Kusu, H.; Ohtaka, A.; Nomura, R. Effect of particle size of DABCO- and DBU- intercalated α-zirconium phosphate as latent thermal catalysts in the reaction of glycidyl phenyl ether (GPE) and hexahydro-4-methylphthalic anhydride (MHHPA). *J. Adhesion Soc. Jpn.* **2018**, *54*, 258−263.
(12) Shimomura, O.; Sasaki, S.; Kume, K.; Ohtaka, A.; Nomura, R. Temperature-Dependent Enhancement Effects for TBD (1,5,7-Triazabicyclo[4.4.0]dec-5-ene) with 2-Methylimidazole-Intercalated α-Zirconium Phosphate as a Latent Thermal Initiator in the Reaction of Glycidyl Phenyl Ether. *Inorganics* **2019**, *7*, 83.
(13) Shimomura, O.; Sasaki, S.; Kume, K.; Ohtaka, A.; Nomura, R. Acceleration effects of 1,5,7-triazabicyclo[4.4.0]dec-5-ene with 2-methylimidazole-intercalated α-zirconium phosphate as a latent thermal initiator in the reaction of glycidyl phenyl ether and hexahydro-4-methylphthalic anhydride. *J. Polym. Sci., Part A: Polym. Chem.* **2019**, *57*, 2557−2561.
(14) Shimomura, O.; Nishisako, T.; Yamaguchi, S.; Ichihara, J.; Kirino, M.; Ohtaka, A.; Nomura, R. DABCO- and DBU-intercalated α-zirconium phosphate as latent thermal catalysts in the copolymerization of glycidyl phenyl ether (GPE) and hexahydro-4-methylphthalic anhydride (MHHPA). *J. Mol. Catal. A: Chem.* **2016**, *411*, 230−238.
(15) Shimomura, O.; Sasaki, S.; Kume, K.; Kawano, S.; Shizuma, M.; Ohtaka, A.; Nomura, R. Release behavior of benzimidazole-intercalated α-zirconium phosphate as a latent thermal initiator in the reaction of epoxy resin. *Catalysts* **2019**, *9*, 69/1−69/13.
(16) Torad, N. L.; Hu, M.; Kamachi, Y.; Takai, K.; Imura, M.; Naito, M.; Yamauchi, Y. Facile synthesis of nanoporous carbons with controlled particle sizes by direct carbonization of monodispersed ZIF-8 crystals. *Chem. Commun.* **2013**, *49*, 2521−2523.
(17) Sadakiyo, M.; Kasai, H.; Kato, K.; Takata, M.; Yamauchi, M. Design and synthesis of hydroxide ion-conductive metal-organic frameworks based on salt inclusion. *J. Am. Chem. Soc.* **2014**, *136*, 1702−1705.
(18) Bhattacharyya, S.; Han, R.; Kim, W.-G.; Chiang, Y.; Jayachandrababu, K. C.; Hungerford, J. T.; Dutzer, M. R.; Ma, C.; Walton, K. S.; Sholl, D. S.; Nair, S. Acid Gas Stability of Zeolitic Imidazolate Frameworks: Generalized Kinetic and Thermodynamic Characteristics. *Chem. Mater.* **2018**, *30*, 4089−4101.
(19) Adhikari, C.; Das, A.; Chakraborty, A. Zeolitic Imidazole Framework (ZIF) Nanospheres for Easy Encapsulation and Controlled Release of an Anticancer Drug Doxorubicin under Different External Stimuli: A Way toward Smart Drug Delivery System. *Mol. Pharmaceutics* **2015**, *12*, 3158−3166.
(20) Armel, V.; Hindocha, S.; Salles, F.; Bennett, S.; Jones, D.; Jaouen, F. Structural Descriptors of Zeolitic-Imidazolate Frameworks Are Keys to the Activity of Fe-N-C Catalysts. *J. Am. Chem. Soc.* **2017**, *139*, 453−464.

https://doi.org/10.1021/acsomega.1c02619
ACS Omega 2021, 6, 30292−30297